Uno *et al.*
Journal of Engineering and Applied Science (2023) 70:137
https://doi.org/10.1186/s44147-023-00311-8

Journal of Engineering and Applied Science

RESEARCH Open Access

Influence of pulse-tail energy of short-pulse CO_2 laser in drilling of various glasses

Kazuyuki Uno[1*], Yasushi Kodama[1,2] and Kazuyuki Yoneya[2]

*Correspondence:
kuno@yamanashi.ac.jp

[1] Integrated Graduate School of Medicine, Engineering, and Agricultural Sciences, University of Yamanashi, Yamanashi, Japan
[2] Seidensha Electronics Co., Ltd. of Japan, 2-2-17 Nishi-Nippori, Arakawa, Tokyo 116-0013, Japan

Abstract

In a short-pulse CO_2 laser based on discharge excitation, there is a pulse tail that depends on the device configuration and operating conditions. The pulse tail is longer than the spike pulse and causes thermal effects such as a crack, heat-affected zones (HAZ), and so on. There are various types of glass having different physical constants related to heat, such as the thermal expansion coefficient and the softening point. Even if the same CO_2 laser pulse is radiated onto glass, the processing results may differ depending on the glass material. Four types of glass, namely, crown glass, soda-lime glass, borosilicate glass, and synthetic quartz glass were irradiated with two types of short CO_2 laser pulses, one with a large pulse tail and one with a small pulse tail, at a repetition rate of 200 Hz and a fluence per pulse of 22 J/cm^2. As the processing characteristics, the ratios of the surface hole diameter and the HAZ diameter to the irradiation diameter, as well as the drilling depth, were investigated. The pulse-tail energy of the short CO_2 laser pulses did not affect the surface hole diameter. In the glasses with small softening points of 740 °C or less, the pulse-tail energy of short CO_2 laser pulses affected the HAZ with a large number of pulse irradiations with a total irradiation fluence of 2000 J/cm^2 or more. The short CO_2 laser pulses with a small tail produced a smaller HAZ than the short CO_2 laser pulses with a large tail. In drilling with a large number of pulse irradiations, the short CO_2 laser pulses with a small tail produced deeper drilling than the short CO_2 laser pulses with a large tail. The glass material did not affect the surface hole diameter and the drilling depth. The glass material affected the HAZ.

Keywords: CO_2 laser, Laser drilling, Glass, Thermal expansion coefficient, Softening point, Crack-less, HAZ

Introduction

Many types of CO_2 lasers have been widely applied in the laser industry because CO_2 lasers can produce pulsed light with a pulse width of 10 ns to 1 ms or continuous wave (CW) light with high power at wavelengths in the range of 9.2 μm to 11.4 μm (mainly 9.6 μm and 10.6 μm). Processing of various materials, such as glass [1–11], polymer resin [12–14], fiber-reinforced resin [15–17], wood [18, 19], etc., by various CO_2 lasers has been reported. In glass processing by a CO_2 laser, the CO_2 laser light is absorbed at the glass surface because the wavelength of a CO_2 laser is 9.2 μm to 11.4 μm. CO_2 lasers employ thermal processing because the pulse width of commercial CO_2 lasers is 10 ns

Springer Open

at the shortest. The heat generated by a laser pulse on a sample may depend on the laser pulse waveform, the pulse width, the fluence, and the repetition rate.

In a transversely excited atmospheric (TEA) CO_2 laser, which is a short-pulse CO_2 laser, the laser pulse waveform has a spike pulse with a width of about 100 ns and a pulse tail with a length of several microseconds [20–24]. Even in our recently developed longitudinally excited CO_2 lasers, the short pulse has a spike pulse with a width of about 100 ns and a pulse tail with a length of several to several hundreds of microseconds, although a short pulse without a pulse tail can be produced [25–29]. Our CO_2 laser controls the spike pulse width and the energy ratio of the spike pulse to the pulse tail. The pulse tail of a discharge-pumped CO_2 laser is caused by a small current after the main discharge and long-lifetime resonance excitation by N_2 contained in the medium gas, and the pulse tail depends on the device configuration and operating conditions. The pulse tail is longer than the spike pulse and causes thermal effects, such as a crack, a heat-affected zone (HAZ), and so on. In our previous work, a short pulse with a spike pulse width of about 250 ns, a pulse tail length of 31.4 μs, and an energy ratio of the spike pulse to the pulse tail of 1:7 to 1:92 produced a crack-less hole in a crown glass with a high thermal expansion coefficient of 100×10^{-7} /K at a repetition rate of 150 Hz to 400 Hz [11]. However, there are various types of glasses, and their physical constants related to heat, such as the thermal expansion coefficient and the softening point, are different. The stress caused by a temperature gradient produces cracks, and glass with a high thermal expansion coefficient tends to crack easily. In addition, glass with a low softening point tends to easily exhibit a HAZ. Therefore, even if the same type of CO_2 laser pulse is used to irradiate different glasses, the processing results may differ depending on the glass material.

In this work, the objective is to investigate the influence of the pulse-tail energy of short-pulse CO_2 laser drilling of various types of glass with thermal expansion coefficients of 100×10^{-7} /K to 5.5×10^{-7}/K and softening points of 724 °C to 1600 °C. Thus, in this work, two types of short CO_2 laser pulses, one with a large tail and one with a small tail, were radiated onto four types of glass with different thermal expansion coefficients and softening points, and the processing characteristics were investigated.

Experimental

Figure 1 shows the schematic diagram of the experimental setup consisting of a longitudinally excited CO_2 laser, an attenuator, a lens, a stage, and a sample [25–29]. The CO_2 laser emitted two types of short laser pulses as shown in Fig. 2. The large-tail short pulse had a spike pulse width of 450 ns, a tail length of 71 μs and an energy ratio of the spike

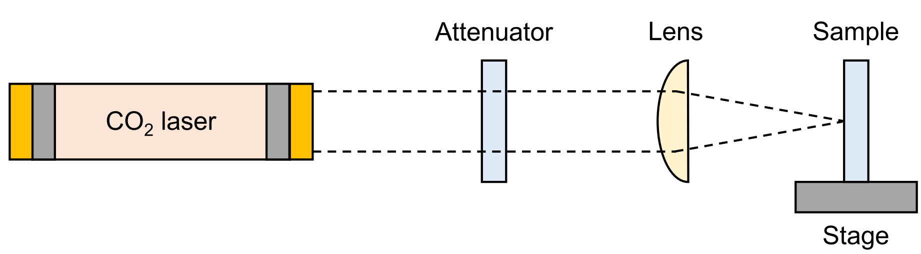

Fig. 1 Schematic diagram of experimental setup

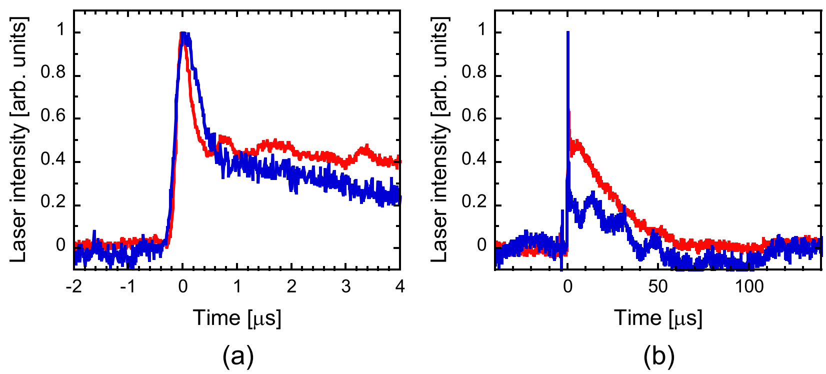

Fig. 2 Laser pulse waveforms. Red and blue lines represent laser pulse waveforms with energy ratios of 1:31 and 1:8, respectively. **a** Magnified time scale of spike pulse. **b** Overall waveform

pulse to the pulse tail of 1:31. The small-tail short pulse had a spike pulse width of 570 ns, a tail length of 35 μs and an energy ratio of the spike pulse to the pulse tail of 1:8. In both laser pulses, the wavelength was 10.6 μm, the repetition rate was 200 Hz, and the beam profile was a circular Gaussian-like shape with a correlation coefficient of 0.98. The focal length of the lens was 38.1 mm, the numerical aperture (NA) was 0.16, and the focal spot size was 230 μm. The sample surface was fixed at the focal plane. The fluence per pulse of whole laser pulse waveforms was adjusted by the attenuator to 22 J/cm^2 in both laser pulse waveforms with energy ratios of 1:31 and 1:8. The samples were crown glass with a thermal expansion coefficient (CTE) of 100×10^{-7}/K, a softening point (SP) of 724 °C and a thickness of 1.1 mm, soda-lime glass with a CTE of 87×10^{-7} /K, a SP of 740 °C and a thickness of 1.2 mm, low expansion borosilicate glass with a CTE of 33×10^{-7}/K, a SP of 820 °C and a thickness of 1.1 mm, and synthetic quartz glass with a CTE of 5.5×10^{-7}/K, a SP of 1600 °C and a thickness of 2.0 mm. As the thermal expansion coefficient decreased, the softening point tended to increase. In CO_2 laser processing of glass with a large thermal expansion coefficient, generally, various treatments before, during, or after irradiation for suppression of crack production have been reported [4–7]. However, in the present work, such treatments were not used to investigate the HAZ.

Results and discussion

In this work, none of the samples exhibited cracks. Figure 3 shows an image of crown glass irradiated with 200 large-tail short pulses with an energy ratio of 1:31. The irradiation diameter was 230 μm, and the total irradiation fluence was 4400 J/cm^2. The surface hole diameter as shown in Fig. 3a was 144 μm, and the ratio of the surface hole diameter to the irradiation diameter was 61.1%. The HAZ diameter as shown in Fig. 3b was 425 μm, and the ratio of the HAZ diameter to the irradiation diameter was 181%. The drilling depth as shown in C of Fig. 3c was 854 μm.

Figure 4 shows the dependence of the ratio of the surface hole diameter to the irradiation diameter on the total irradiation fluence, that is the fluence per single pulse multiplied by the number of irradiation pulses in crown glass with a CTE of 100×10^{-7}/K and a SP of 724 °C, soda-lime glass with a CTE of 87×10^{-7}/K and SP of 740 °C, low expansion borosilicate glass with a CTE of 33×10^{-7}/K and a SP of 820 °C, and synthetic quartz glass with a CTE of 5.5×10^{-7}/K and a SP of 1600 °C. In

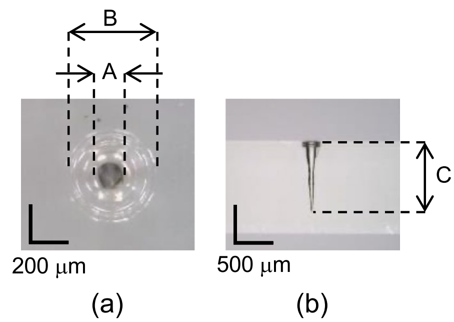

Fig. 3 Image of crown glass irradiated with 200 short pulses with a large tail **a** Surface image. **a** and **b** show surface hole diameter and HAZ diameter, respectively. **b** Side image. **c** shows the drilling depth

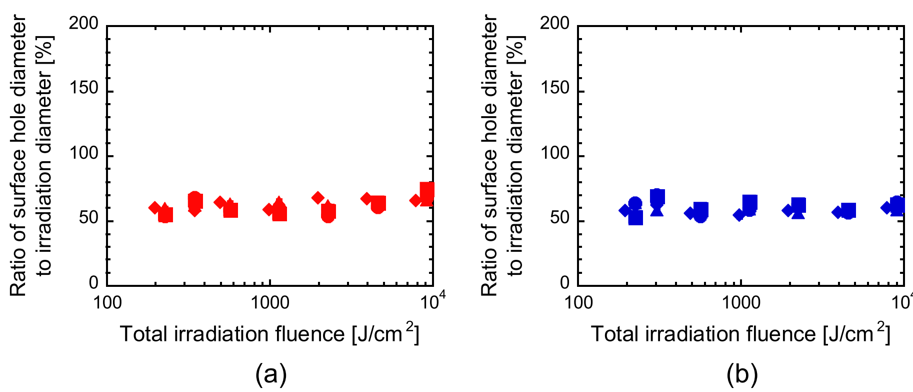

Fig. 4 Dependence of ratio of surface hole diameter to irradiation diameter on total irradiation fluence. Circles, squares, diamonds, and triangles represent crown glass, soda-lime glass, borosilicate glass, and synthetic quartz glass, respectively. **a** Laser pulse waveform with an energy ratio of 1:31. **b** Laser pulse waveform with an energy ratio of 1:8

this work, the results were presented using the ratio of the surface hole diameter to the irradiation diameter to illustrate the relationship between the irradiation diameter and the surface hole diameter. Figure 4a presents the results obtained with the large-tail short laser pulse with the energy ratio of the spike pulse to the pulse tail of 1:31, and Fig. 4b presents the results obtained with the small-tail short laser pulse the energy ratio of 1:8. In the laser pulse waveform with the energy ratio of 1:31, the ratio of the surface hole diameter increased slightly with the increase of the total irradiation fluence but did not depend on the glass material. The average ratio was about 59.8%. In the laser pulse waveform with the energy ratio of 1:8, the ratio of the surface hole diameter did not depend on the total irradiation fluence or the glass material and was constant at about 59.8%.

Figure 5 shows the dependence of the ratio of the HAZ diameter to the irradiation diameter on the total irradiation diameter in crown glass with a CTE of 100×10^{-7} /K and a SP of 724 °C, soda-lime glass with a CTE of 87×10^{-7}/K and SP of 740 °C, low expansion borosilicate glass with a CTE of 33×10^{-7}/K and a SP of 820 °C, and synthetic quartz glass with a CTE of 5.5×10^{-7} /K and a SP of 1600 °C. In this work, the results were presented using the ratio of the HAZ diameter to the irradiation diameter to illustrate the relationship between the irradiation diameter and the HAZ

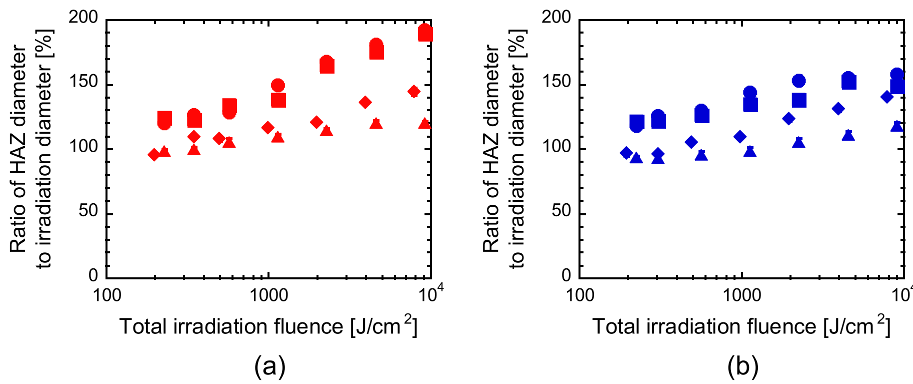

Fig. 5 Dependence of ratio of HAZ diameter to irradiation diameter on total irradiation fluence. Circles, squares, diamonds, and triangles represent crown glass, soda-lime glass, borosilicate glass, and synthetic quartz glass, respectively. **a** Laser pulse waveform with an energy ratio of 1:31. **b** Laser pulse waveform with an energy ratio of 1:8

diameter. Figure 5a presents the results obtained with the large-tail short laser pulse with the energy ratio of the spike pulse to the pulse tail of 1:31, and Fig. 5b presents the results obtained with the small-tail short laser pulse with the energy ratio of 1:8. In both laser pulse waveforms with the energy ratios of 1:31 and 1:8, the ratio of the HAZ diameter increased with the increase of the total irradiation fluence, and the decrease of the softening point of the glass. The ratio of the HAZ diameter produced by the laser pulse waveform with the energy ratio of 1:31 was larger than that produced by the laser pulse waveform with the energy ratio of 1:8. In particular, in a glass material with a low softening point, the difference became significant when the total irradiation fluence was over 2000 J/cm^2.

Figure 6 shows the dependence of the drilling depth on the total irradiation diameter in crown glass with a CTE of 100×10^{-7}/K and a SP of 724 °C, soda-lime glass with a CTE of 87×10^{-7}/K and SP of 740 °C, low expansion borosilicate glass with a CTE of 33×10^{-7}/K and a SP of 820 °C, and synthetic quartz glass with a CTE of 5.5×10^{-7}/K and a SP of 1600 °C. Figure 6a presents the results obtained with the large-tail short laser pulse with the energy ratio of the spike pulse to the pulse tail of 1:31, and Fig. 6b

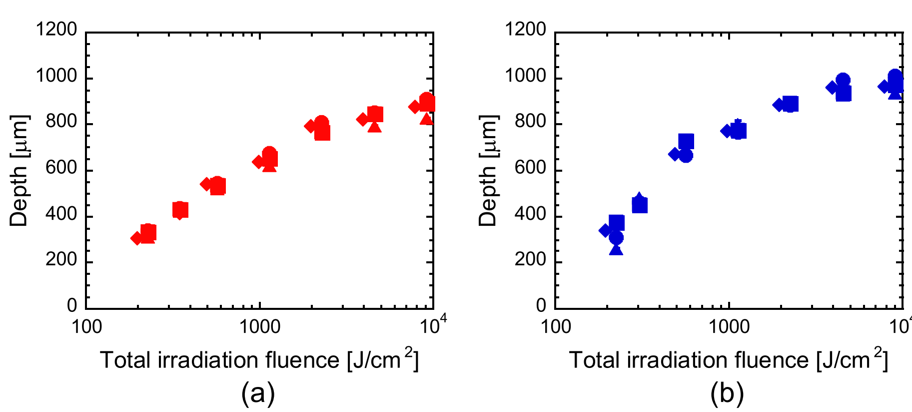

Fig. 6 Dependence of drilling depth on total irradiation fluence. Circles, squares, diamonds, and triangles represent crown glass, soda-lime glass, borosilicate glass, and synthetic quartz glass, respectively. **a** Laser pulse waveform with an energy ratio of 1:31. **b** Laser pulse waveform with an energy ratio of 1:8

presents the results obtained with the small-tail short laser pulse with the energy ratio of 1:8. In both laser pulse waveforms with the energy ratios of 1:31 and 1:8, the drilling depth increased with the increase of the total irradiation fluence but did not depend on the glass material. At a total irradiation fluence of about 220 J/cm^2, the drilling depth produced by the laser pulse waveform with the energy ratio of 1:31 was almost the same as that produced by the laser pulse waveform with the energy ratio of 1:8 and was about 323 μm. However, at a total irradiation fluence of 500 J/cm^2 or more, the drilling depth produced by the laser pulse waveform with the energy ratio of 1:31 was smaller than that produced by the laser pulse waveform with the energy ratio of 1:8. This may be attributed to the fluence of the spike pulse part of the laser pulse waveform. In this work, the fluence per single pulse of whole laser pulse waveforms was 22 J/cm^2 in both laser pulse waveforms with the energy ratios of 1:31 and 1:8. Therefore, the fluence per pulse of the spike pulse parts was 0.69 J/cm^2 and 2.44 J/cm^2 in the laser pulse waveforms with the energy ratios of 1:31 and 1:8, respectively. In drilling with a large number of irradiation pulses, the fluence per pulse of the spike pulse part affected the drilling depth.

Conclusions

Two types of short CO_2 laser pulses, with a large or small tail, were radiated onto four types of glass with thermal expansion coefficients of 100×10^{-7}/K to 5.5×10^{-7}/K and softening points of 724 °C to 1600 °C at a repetition rate of 200 Hz and a fluence per pulse of 22 J/cm^2, and the processing characteristics, in terms of the ratios of the surface hole diameter and the HAZ diameter to the irradiation diameter, as well as the drilling depth, were investigated. The surface hole diameter did not depend on the pulse-tail energy of the short CO_2 laser pulse and the glass material. The ratio was about 59.8%. In glass with a large softening point of 820 °C or more, the HAZ was not affected by the pulse-tail energy of a short CO_2 laser pulse. In glass with a small softening point of 740 °C or less, the HAZ produced by the short CO_2 laser pulse with a small tail at a total irradiation fluence of 2000 J/cm^2 or more was smaller. The drilling depth increased with the increase of the total irradiation fluence but did not depend on the glass material. In drilling with a large number of irradiation pulses, the fluence per pulse of the spike pulse part affected the drilling depth. Therefore, in glass processing by a short-pulse CO_2 laser, the pulse-tail energy of the laser pulse waveform is an important parameter to be considered. However, with a small total irradiation fluence produced by a small number of irradiation pulses, the pulse-tail energy of the laser pulse waveform does not affect the results of glass drilling.

Abbreviations

CO_2	Carbon dioxide
HAZ	Heat affected zone
CW	Continuous wave
TEA	Transversely excited atmospheric
NA	Numerical aperture
CTE	Thermal expansion coefficient
SP	Softening point

Acknowledgements

This research was partially supported by the Japan Science and Technology Agency for A-STEP, AS3015041S. The authors wish to thank Yoshihito Baba in our group.

Authors' contributions
All authors have contributed to this research. The conception of the study, data collection, and manuscript draft were done by KU. The acquisition and material preparation were done by YK and KY. All authors read and approved the final manuscript.

Funding
The authors declare that no funds, grants, or other support were received during the preparation of this manuscript.

Availability of data and materials
The datasets generated during the current study are available from the corresponding author on reasonable request.

Declarations

Competing interests
The authors declare that they have no competing interests.

Received: 30 January 2023 Accepted: 31 October 2023
Published online: 13 November 2023

References

1. Ogura H, Yoshida Y (2003) Hole Drilling of Glass Substrates with a CO_2 Laser. Jpn J Appl Phys 42:2881–2886
2. Nowak KM, Baker HJ, Hall DR (2015) Analytical model for CO_2 laser ablation of fused quartz. App Optics 54:8653–8663
3. Zhang C, Zhang L, Jiang X, Jia B, Liao W, Dai R, Chen J, Yuan X, Jiang X (2020) Influence of pulse length on heat affected zones of evaporatively-mitigated damages of fused silica optics by CO_2 laser. Opt Laser Eng 125:105857
4. Brusberg L, Queisser M, Gentsch C, Schroder H, Lang KD (2012) Advances in CO_2-Laser Drilling of Glass Substrates. Phys Procedia 39:548–555
5. Chung CK, Lin SL (2010) CO_2 laser micromachined crackles through holes of Pyrex 7740 glass. Int J Mach Tools Manuf 50:961–968
6. Ali A, Sundaram M (2018) Drilling of crack free micro holes in glass by chemo-thermal micromachining process. Precis Eng 54:33–38
7. Chung CK, Lin SL, Wang HY, Tan TK, Tu KZ, Lung HF (2013) Fabrication and simulation of glass micromachining using CO_2 laser processing with PDMS protection. Appl Phys A 113:501–507
8. Kim T, Kwan KK, Chu CN, Song KY (2020) Experimental investigation on CO_2 laser-assisted micro-slot milling characteristics of borosilicate glass. Precis Eng 63:137–1477
9. Perrone E, Cesaria M, Zizzari A, Bianco M, Ferrara F, Raia L, Guarino V, Cuscuna M, Mazzeo M, Gigli G, Moroni L, Arima V Potential of CO_2-laser processing of quartz for fast prototyping of microfluidic reactors and templates for 3D cell assembly over large scale. Mater. Today Bio 12:100163.
10. Furumoto T, Hashimoto Y, Ogi H, Kawabe T, Yamaguchi M, Koyano T, Hosokawa, (2021) A CO_2 laser cleavage of chemically strengthened glass. J Mater Process Technol 289:116961
11. Rahaman ME, Uno K (2022) Crown glass drilling by short-pulse CO_2 laser with tunable pulse tail. Lasers Manuf Mater Process 9:72–80
12. Prakash S, Kumar S (2021) Determining the suitable CO_2 laser based technique for microchannel fabrication on PMMA. Opt Laser Technol 139:107017
13. Kaba AM, Jeon H, Park A, Yi K, Baek S, Park A, Kim D (2021) Cavitation-microstreaming-based lysis and DNA extraction using a laser-machined polycarbonate microfluidic chip. Sens Actuators B Chem 346:130511
14. Abdulwahab AE, Hubeatir KA, Imhan KI (2022) Optimization of PC micro-drilling using a continuous CO_2 laser: am experimental and theoretical comparative study. J Eng Appl Sci 69:98
15. Salama A, Li L, Mativenga P, Whitehead D (2016) TEA CO_2 laser machining of CFRP composite. Appl Phys A 122:497
16. Endo M, Araya N, Kurokawa Y, Uno K (2016) Anomalous enhancement of drilling rate in carbon fiber reinforced plastic using azimuthally polarized CO_2 laser. Laser Phys 26:096001
17. Solati A, Hamedi M, Safarabadi M (2019) Comprehensive investigation of surface quality and mechanical properties in CO_2 laser drilling of GFRP composites. Int J Adv Manuf Technol 102:791–808
18. Nath S, Waugh DG, Ormondroyd GA, Spear MJ, Pitman AJ, Sahoo S, Curling SF, Mason P (2020) CO_2 laser interactions with wood tissues during single pulse laser-incision. Opt Laser Technol 126:106069
19. Guo X, Deng M, Hu Y, Wang Y, Ye T (2021) Morphology, mechanism and kerf variation during CO_2 laser cutting pine wood. J Manuf Process 68:13–22
20. Menyuk N, Moulton PF (1980) Development of a high-repetition-rate mini-TEA CO_2 laser. Rev Sci Instrum 51:216
21. Karapuzikov AI, Malov AN, Sherstov IV (2000) Tunable TEA CO_2 laser for long-range DIAL lidar. Infrared Phys Technol 41:77–85
22. Wu J, Zhang Z, Wang D, Liu S, Tang Y, Tan R, Zhang K, Wan C (2007) Novel long-pulse TE CO_2 laser excited by pulser-sustainer discharge. Opt Laser Technol 39:701–704
23. Bellecci C, Gaudio P, Martellucci S, Penco E, Richetta M (2005) Active clipping system for transversely excited CO_2 lasers. Rev Sci Instrum 76:026115
24. Hurst N, Harilal SS (2009) Pulse shaping of transversely excited atmospheric CO_2 laser using a simple plasma shutter. Rev Sci Instrum 80:035101
25. Uno K, Jitsuno T (2018) Control of laser pulse waveform in longitudinally excited CO_2 laser by adjustment of excitation circuit. Opt Laser Technol 101:195–201

26. Uno K, Jitsuno T (2018) Control of laser pulse waveform in longitudinally excited CO_2 laser by adjustment of gas medium. Proc SPIE 10811:1081111
27. Uno K, Li J, Goto H, Jitsuno T (2018) Longitudinally excited CO_2 laser with short laser pulse and high quality beam. Proc SPIE 10518:105181Y
28. Sakamoto K, Uno K, Jitsuno T (2019) Longitudinally excited CO_2 laser with a spike pulse width of 100 ns to 300 ns. Proc SPIE 10898:108980U
29. Uno K, Yanai K, Watarai S, Kodama Y, Yoneya K, Jitsuno T (2022) 1 kHz Oscillation of short-pulse CO_2 laser pumped by longitudinal discharge without pre-ionization. Opt Laser Technol 152:108174

Publisher's Note